

# Global evidence of rapid urban growth in flood zones since 1985

<https://doi.org/10.1038/s41586-023-06468-9>

Received: 17 March 2022

Accepted: 21 July 2023

Published online: 4 October 2023

 Check for updates

Jun Rentschler<sup>1</sup>✉, Paolo Avner<sup>1</sup>, Mattia Marconcini<sup>2,3</sup>, Rui Su<sup>1</sup>, Emanuele Strano<sup>3</sup>, Michalis Vousdoukas<sup>4</sup> & Stéphane Hallegatte<sup>1</sup>

Disaster losses are increasing and evidence is mounting that climate change is driving up the probability of extreme natural shocks<sup>1–3</sup>. Yet it has also proved politically expedient to invoke climate change as an exogenous force that supposedly places disasters beyond the influence of local and national authorities<sup>4,5</sup>. However, locally determined patterns of urbanization and spatial development are key factors to the exposure and vulnerability of people to climatic shocks<sup>6</sup>. Using high-resolution annual data, this study shows that, since 1985, human settlements around the world—from villages to megacities—have expanded continuously and rapidly into present-day flood zones. In many regions, growth in the most hazardous flood zones is outpacing growth in non-exposed zones by a large margin, particularly in East Asia, where high-hazard settlements have expanded 60% faster than flood-safe settlements. These results provide systematic evidence of a divergence in the exposure of countries to flood hazards. Instead of adapting their exposure, many countries continue to actively amplify their exposure to increasingly frequent climatic shocks.

The world's cities are growing rapidly as people from peripheral regions move in search of economic opportunities<sup>7</sup>. Urbanization and economic development have traditionally gone hand in hand as cities enable agglomeration economies<sup>8</sup>, for instance, by matching employers and job seekers, sellers and buyers, and capital and projects, and supporting productive infrastructure such as public transport systems<sup>9,10</sup>.

However, rapid urban growth can also cause congestion effects; for instance, by increasing exposure to natural hazards and pressure on public services and infrastructure. This is particularly relevant in low-income and middle-income countries that lack the capacity for risk-informed urban and infrastructure planning and the resources to invest in transport and protection infrastructure. Moreover, spaces that are safe from floods are increasingly occupied and the resulting land scarcity can drive new developments disproportionately into previously avoided areas, including riverbeds and floodplains (Fig. 1).

Despite the increasing interplay between rapid urbanization trends and flood disasters, the lack of high-resolution flood-hazard maps and annual settlement footprint data has been a key factor limiting systematic analysis of global flood-exposure trends<sup>11</sup>. By using historical records of flood events, such as EM-DAT, studies have estimated exposure indicators at the country level<sup>12</sup>. However, lacking information on the spatial distribution of flood hazards and populations means that continuously evolving urban shapes cannot be taken into account accurately, thus making flood exposure difficult to compare over time<sup>11,13,14</sup>. A study based on satellite imagery from 2000 to 2018 offered important insights on the growing populations affected by floods<sup>7</sup>. Although such imagery can detect many past floods, it does not shed light on the underlying spatial expansion and exposure patterns of all human settlements. The number of people who were affected by floods between 2000 and 2018 represents a small share of the overall at-risk populations<sup>15</sup>.

Owing to data limitations, past studies also focus on certain types of flood, rather than assessing the combined hazards from all flood types (that is, fluvial, pluvial and coastal flooding)<sup>11,14,16–18</sup>. Others assess hazards for a subset of countries, falling short of full global coverage<sup>19,20</sup>. Similarly, studies using relatively coarse spatial resolution flood-hazard data tend to inaccurately represent principal floodplains, thus underestimating exposure<sup>19,21–25</sup>.

This study makes several contributions. First, by considering flood-exposure trends with annual frequency, it demonstrates the value of continuous monitoring of evolving flood exposure. Second, it distinguishes the growth dynamics of flood-exposed versus flood-safe spatial development to document a divergence in flood exposure—regions that are either increasing or decreasing exposure as they urbanize. Third, rather than focusing on a certain flood type, it combines different flood types and assesses overall exposure. Fourth, by using high-resolution global datasets, it documents trends with complete global coverage and within one consistent methodology. Last, by estimating spatially disaggregated trends of urbanization and flood exposure, it offers concrete evidence to policymakers for prioritizing measures in risk prevention, reduction and preparedness.

## Globally, urbanization is more rapid in flood-prone areas

This study shows that, in 2015, at least 11.3% of all built-up areas globally face high or very high flood hazards; that is, inundation depths of at least 50 cm during 1-in-100-year flood events (Extended Data Table 1). Exposure is lowest in Sub-Saharan Africa (4.6%) and North America (4.5%) and highest in the East Asia and Pacific region (18.4%). Overall, flood-exposure levels are substantial across all global regions and income groups.

<sup>1</sup>The World Bank, Washington, DC, USA. <sup>2</sup>German Aerospace Center (DLR), Munich, Germany. <sup>3</sup>MindEarth, Biel, Switzerland. <sup>4</sup>Department of Marine Sciences, University of the Aegean, Mytilene, Greece. ✉e-mail: jrentschler@worldbank.org

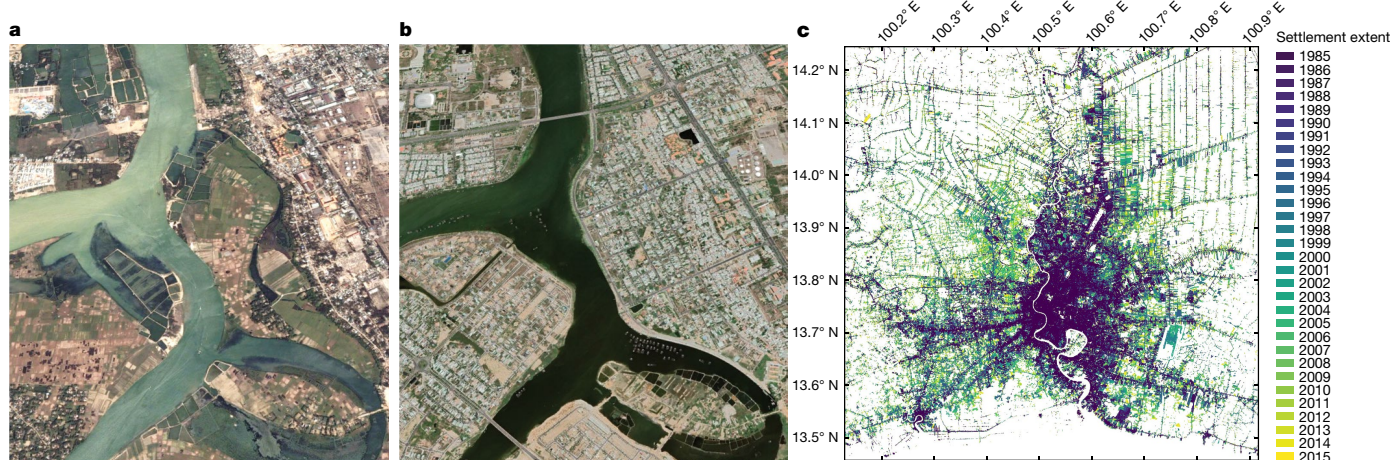


**Fig. 1 | Riverside-settlement expansion.** **a,b**, Satellite imagery from Quang Nam, Vietnam, in 2002 (**a**) and 2021 (**b**) (source: Google Earth, Maxar Technologies). **c**, WSF-Evo settlement footprints for Bangkok, Thailand, between 1985 and 2015 (source: DLR).

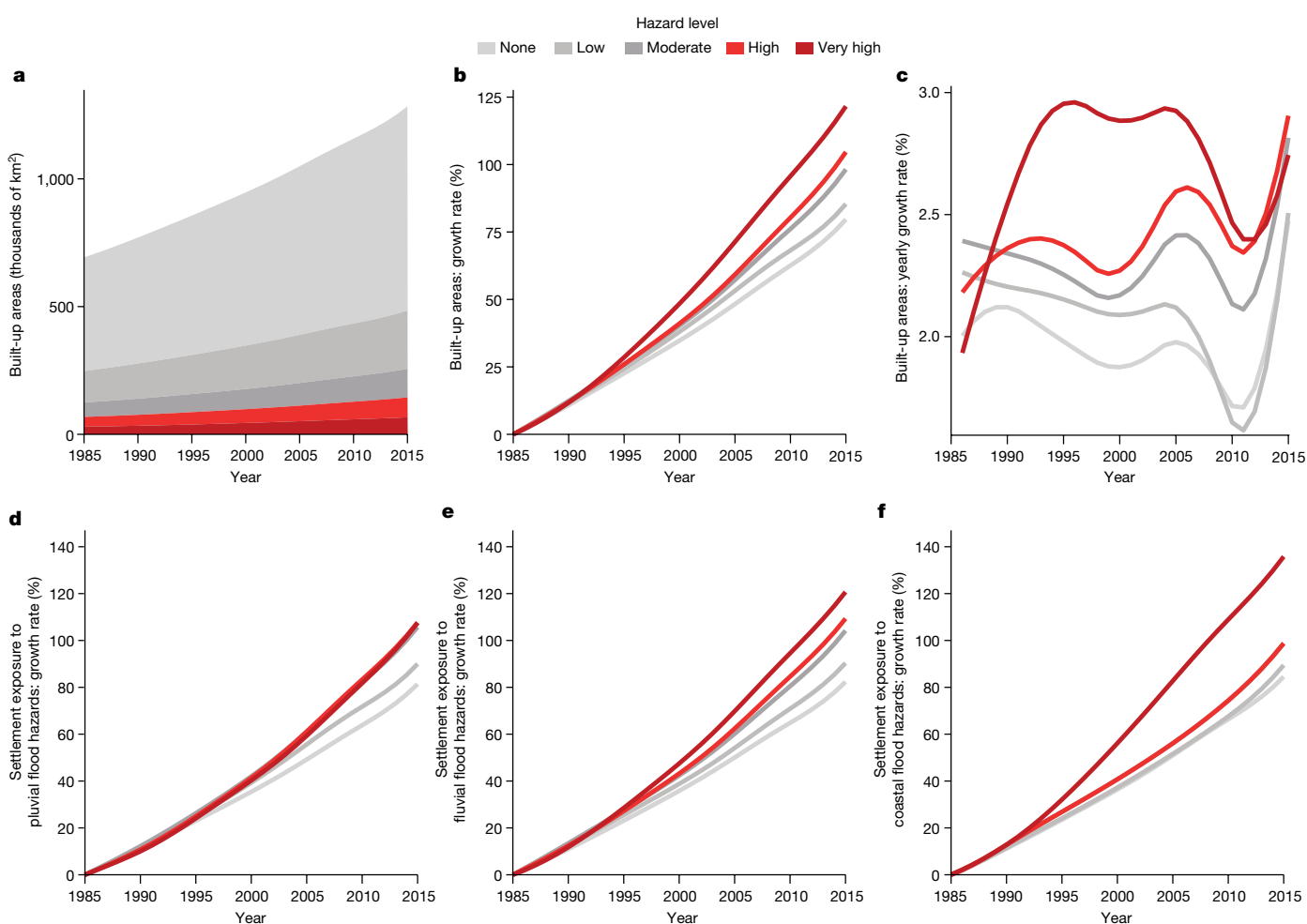


**Fig. 2 | Global settlement growth is fastest where hazards are highest.** Panels show the global evolution of settlement expansion at different combined flood-hazard levels in absolute terms (**a**), 1985 to 2015 percentage growth (**b**) and year-on-year growth rates (**c**). Panels **d–f** disaggregate combined flood hazards into pluvial floods (**d**), fluvial floods (**e**) and coastal

floods (**f**). Hazard classes are defined on the basis of the estimated inundation depth during a 1-in-100-year flood: none (flood depths of 0 cm), low (up to 15 cm), moderate (between 15 and 50 cm), high (between 50 and 150 cm) and very high (over 150 cm).

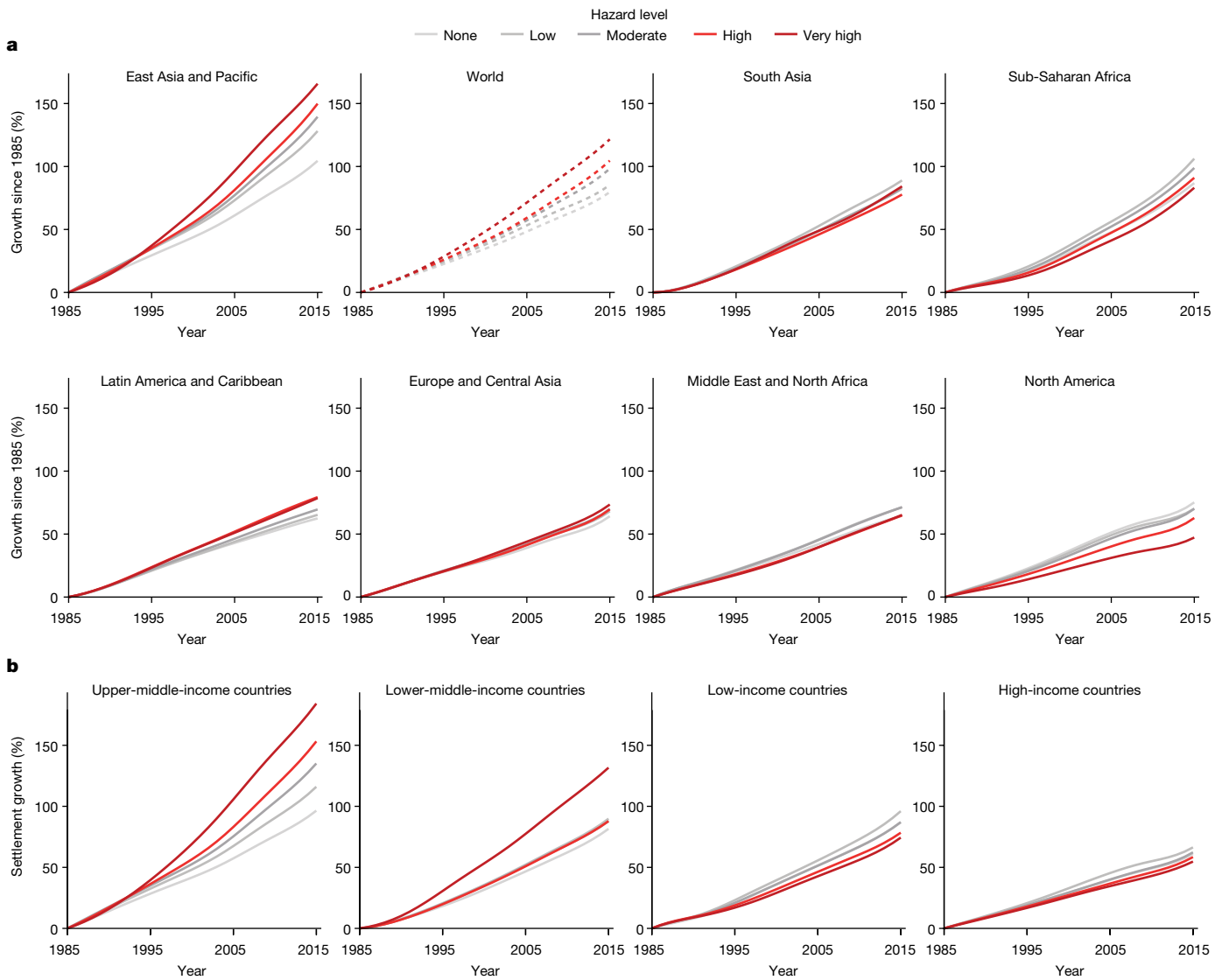


**Fig. 3 | Settlement growth by hazard level.** Panels show the evolution of settlement expansion at different combined flood-hazard levels in different world regions (a) and income groupings (b). Charts are sorted from fastest to slowest high-hazard growth.

Between 1985 and 2015, the world's built-up settlements grew by 85%, from 693,000 to more than 1.28 million square kilometres. At the same time, the share of settlements in flood-safe areas dropped by 1.9 percentage points and the share in higher-hazard categories increased (Extended Data Table 1). In 2015, 20% of all settlement areas were in zones with medium or higher flood hazards, up from 17.9% in 1985. The share in the highest-hazard category has grown most, from 4.3% to 5.2%. Of the land that has been built up since 1985, more than 36,500 square kilometres face inundation depths of over 1.5 m during severe flood events—equivalent to 23 times the area of Greater London—and 76,400 square kilometres are exposed to inundation over 0.5 m.

Settlement expansion in high-hazard flood zones outpaces growth in flood-safe areas. Although the world's overall settlement extent has increased by 85.4%, settlements with high flood-hazard exposure have grown by 105.8% and those exposed to the highest flood-hazard level by 121.6% (Fig. 2b). Year-on-year growth estimates confirm that, since the early 1990s, settlement growth in the highest-hazard flood category has increased by almost 3% a year, consistently outpacing flood-safe growth (Fig. 2c). The 2007–2010 slowdown in settlement expansion coincides with a global recession. Flood-exposed settle-

ment growth is outpacing flood-safe growth regardless of which flood type is considered, although exposure to coastal floods is growing most rapidly (Fig. 2d–f).

### East Asia has the highest increase in exposure

Urbanization and flood-exposure dynamics differ markedly across regions. The East Asia and Pacific region stands out with the highest urban growth rate and the largest proportion of settlements in the highest flood-hazard category (inundation depth over 1.5 m; Extended Data Fig. 1). Between 1985 and 2015, 'no hazard' settlements expanded by just over 100%, whereas 'very high hazard' settlements expanded by over 160% (Fig. 3a).

Flood-exposed growth is outpacing non-exposed growth in Latin America and the Caribbean, Europe and Central Asia, and East Asia and Pacific, whereas in Sub-Saharan Africa, North America, and Middle East and North Africa, the opposite is true (Fig. 3a). In North America, flood-safe settlements expanded by 75%, compared with 49% in the highest-hazard zones. However, even in these regions, settlements in high-hazard flood zones have continuously expanded, exposing an ever-growing number of people and assets. Regionally

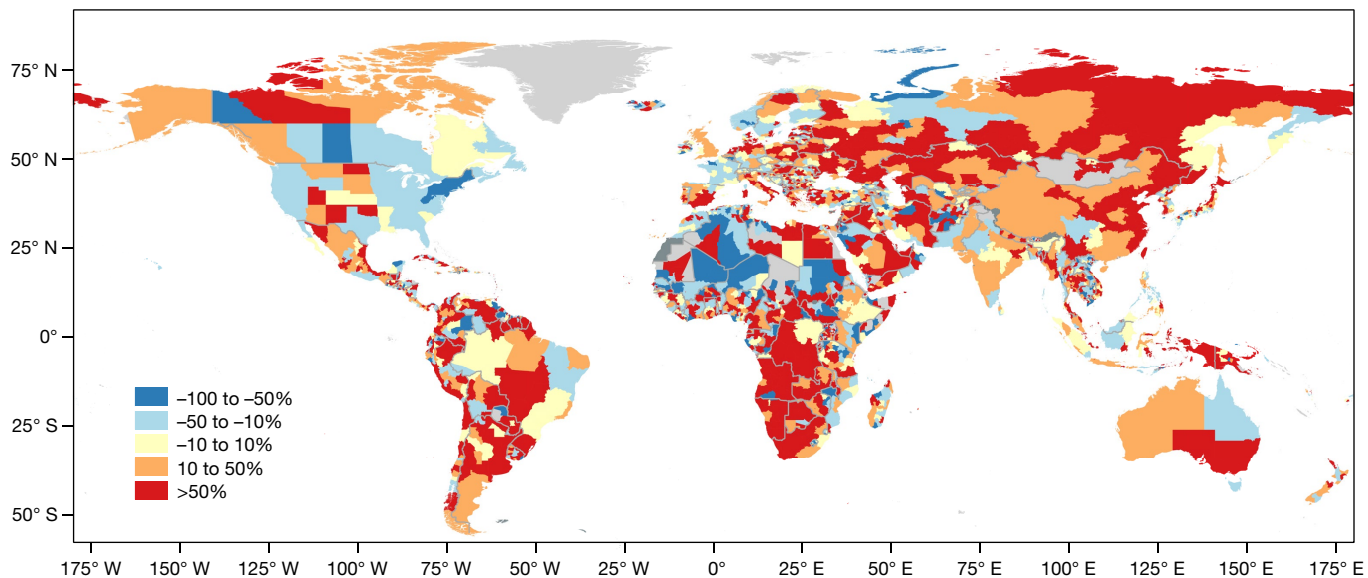


**Fig. 4 | Flood-safe versus flood-exposed growth: relative difference between settlement growth in safe and high-hazard areas from 1985 to 2015.** In red areas, the share of flood-exposed settlements is increasing, that is,

settlements in high-hazard flood zones have expanded at least 50% more than settlements in flood-safe areas. In blue areas, flood exposure is decreasing.

disaggregated year-on-year growth rates show that settlement expansion fluctuates across time and regions between 1% and 4% (Extended Data Fig. 2), apparently driven by a range of factors, including economic fundamentals.

### A growing divergence in flood exposure

Country income groupings further clarify urbanization and flood-hazard patterns (Fig. 3b). Of the 36,500 square kilometres of settlements built in highest-hazard zones since 1985, 1.1% are in low-income countries (LICs), 20.5% are in lower-middle-income countries (LMICs), 60.8% are in upper-middle-income countries (UMICs) and 17.6% are in high-income countries (HICs).

MICs have seen the fastest urban growth since 1985, hosting 72% of the world's 144,600 square kilometres of built-up areas in high-hazard flood zones in 2015. On average, growth in high-hazard flood zones is outpacing growth in flood-safe zones by large margins (Fig. 3b). In LMICs, settlements in highest-hazard areas expanded by 132% since 1985, compared with 86% of overall settlement expansion. These expanding settlements in high-hazard areas lock in flood exposure, as well as future losses and the need for mounting flood-protection investments. UMICs have a higher proportion of settlements in the highest-hazard areas than any other group. Since 1985, these have grown by 184%—nearly twice the rate of flood-safe settlements (96%).

In comparison, LICs have seen moderate settlement growth since 1985. The difference in growth in flood-safe (87%) and high-hazard or very-high-hazard areas (77%) is less pronounced than in MICs. On average, settlement growth in high-hazard areas has not outpaced flood-safe growth, although this trend risks reversing in the future as economic growth and urbanization accelerate.

Settlement expansion has been the slowest in HICs (62%), coinciding with comparably slow economic and population growth rates. However, many HICs experienced periods of rapid urban expansion before 1985. On average, urban growth in flood-safe areas has been faster than in high-hazard areas (Fig. 3b).

Overall, these results indicate a divergence in the exposure of countries to flood hazards. Although flood-safe growth dominates in some countries, others are actively increasing their relative exposure to flood

hazards. Subnationally disaggregated results show that this divergence is also occurring within countries across all regions (Fig. 4).

The substantial increase in flood exposure in UMICs is driven by settlement expansion in China. Between 1985 and 2015, built-up areas in China increased by 165%, with settlements in the highest flood-hazard category growing by 223%. Country-specific studies have already documented this trend, finding a rapid increase in flood exposure and damages, especially around the main metropolitan areas in the northeast and coastal regions<sup>26–29</sup>.

With larger settlement areas than any other country (Extended Data Fig. 3a), China contributes substantially to the trends observed for both MICs and the East Asia and Pacific region. With 46% of the world's 76,400 square kilometres of new high-hazard settlements within its borders, China is the largest contributor to the global expansion of high-hazard settlements. Vietnam and Bangladesh also stand out as LMICs with large settlement areas exposed to the highest flood-hazard category (Extended Data Fig. 3c).

Although they have seen relatively slow and flood-safe growth in the past 30 years, many HICs, including Japan, the USA and the Netherlands, already had large settlement areas in high-hazard flood zones in 1985 and have invested heavily in protecting them (Extended Data Fig. 3b). In the Netherlands, sea dykes protect against up to 1-in-10,000-year storm surges. Nevertheless, even in HICs, many settlements are not protected against the 1-in-100-year flood hazards considered in this study. Recent disasters—including in the USA, the UK and Germany—show that floods continue to pose substantial risks to lives, livelihoods and assets.

The results also identify smaller countries that face disproportionately high exposure. In three-quarters of all countries, 4% or less of overall settlements are estimated to be high-hazard settlements, but in several countries, exposure shares are much higher. Figure 5 presents the top 20 countries in terms of flood-exposed settlement shares. In the Netherlands, more than 35% of all settlements are in high-hazard zones in terms of hydrology and elevation, although these risks are mitigated through advanced (but not infallible) protection infrastructure. The same is not true in most LICs and MICs, such as Laos (34%) and Vietnam (25.4%), in which many settlements are highly exposed without strong protection systems. Flood exposure is particularly high for countries in which settlements concentrate along river valleys and

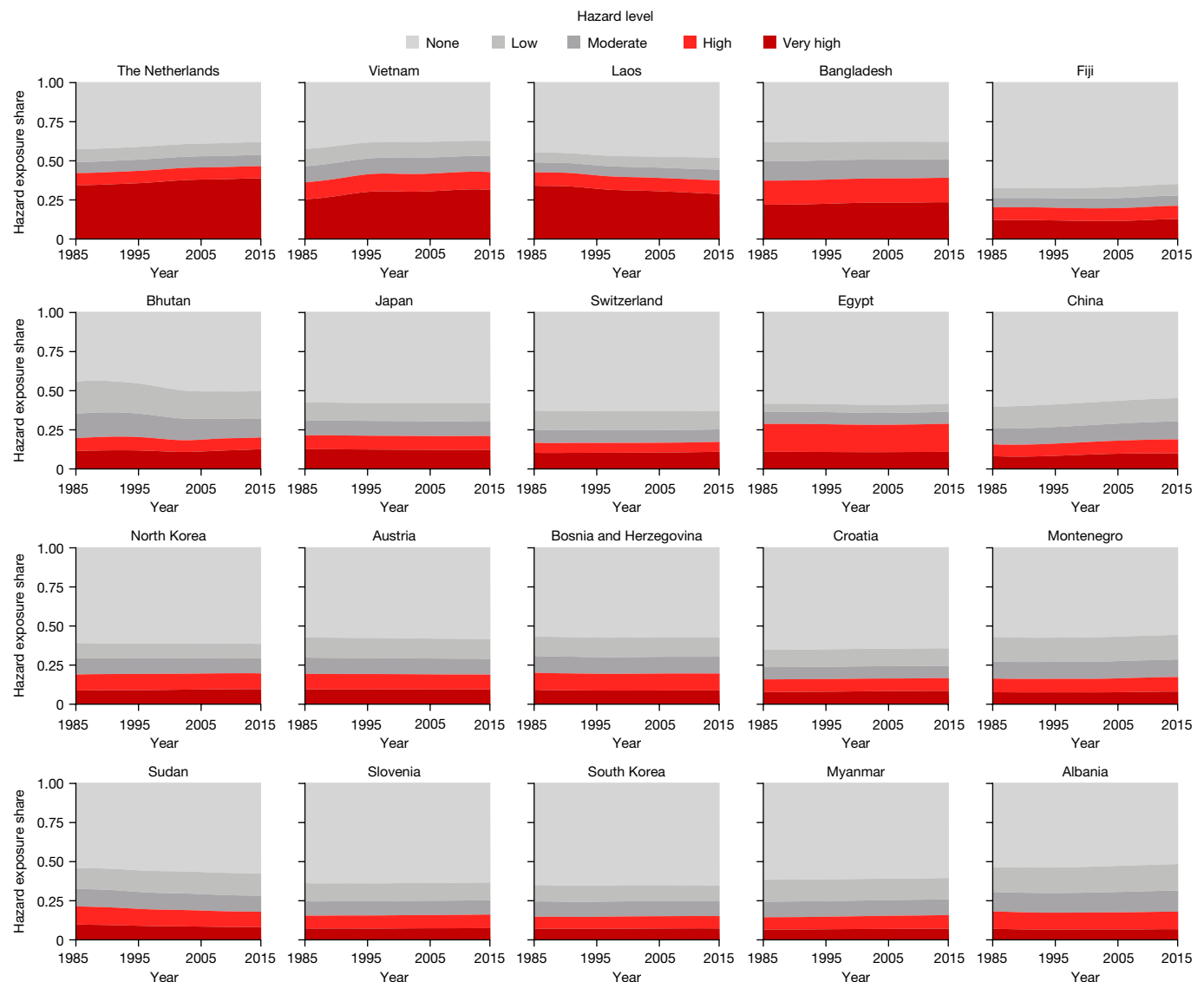


**Fig. 5 | Top 20 countries in terms of settlement area by flood-hazard level.** Countries are ranked by their share of ‘very high’ hazard exposure, showing the evolution of the exposure share from 1985 to 2015. Countries with populations under 100,000 are omitted from this figure.

basins (such as Bhutan, Egypt and Bangladesh) and coastal areas (such as Fiji and Vietnam).

### Urbanization in a changing climate

Climate change forces countries to adapt to intensifying natural hazards. However, efforts to track the success of countries in adaptation have proved difficult or even misleading<sup>30</sup>. Besides the changing climate itself, the exposure of people to climate hazards is also determined locally by spatial development choices. Demographic and economic growth is accompanied by migration from rural to urban areas, resulting in urban expansion as new neighbourhoods and industrial parks spring up, often in flood zones. Moreover, the vulnerability of people to climatic shocks is determined in a complex context of social, economic, institutional and historical factors.

This study documents a divergence in the exposure of countries to flood hazards. Rather than adapting their exposure to climatic hazards, many countries are actively increasing it. Although growth is shown to be relatively flood-safe in HICs, flood-exposed growth has been especially rapid in MICs—and LICs may risk following this trajectory in the future. These trends suggest the influence of a variety of potential

underlying drivers for the increasing flood exposure of urbanization, including land scarcity, socioeconomic trends and institutional and regulatory factors.

Risks are exacerbated when urban planning fails to assign priority to densification of safe areas to avoid expanding into hazardous zones. For instance, in Vietnam, where almost one-third of the coastline is now built up, the safest and most productive locations are increasingly occupied; thus, new developments are disproportionately forced onto hazardous land and previously avoided areas, such as riverbeds or floodplains<sup>31</sup>. Evidence from the US Atlantic coast documents how, in recent decades, new construction avoided flood-prone areas in sparse locations but took place in the ‘least bad’ flood-prone areas in dense locations<sup>32</sup>.

When making locational decisions, households and businesses often trade off job accessibility and market potential with disaster risks, and settling in flood-prone areas can become a rational choice<sup>33</sup>. However, behavioural biases, market failures and information constraints can exacerbate excessive risk-taking. Inefficient land markets can allow safe land to sit idle while hazardous areas are developed. In informal low-income settlements, physical flood risks are often exacerbated by a lack of public infrastructure (including drainage) and social support systems<sup>6</sup>.

# Article

This study shows that these cases and mechanisms reflect a global trend. Especially in MICs—with their rapidly growing economies and urban centres—settlement growth in flood zones is outpacing growth in flood-safe areas. And, globally, overall settlements expanded by 85% between 1985 and 2015 on average, whereas those exposed to the highest flood-hazard level increased by 122%.

These findings carry concrete implications for urban planners and policymakers. In areas in which flood exposure is already high, investments in disaster preparedness are crucial to mitigate losses. In areas in which flood exposure is still low but increasing rapidly, revision of land use and urbanization plans is urgent, along with updating risk-informed building codes and infrastructure master plans. Although land scarcity and geographic constraints may mean that settling in flood zones cannot always be avoided, flood-protection systems and disaster-preparedness measures can still support resilient socio-economic development. As well as addressing exposure, it is crucial to address underlying drivers of the vulnerability of people.

## Online content

Any methods, additional references, Nature Portfolio reporting summaries, source data, extended data, supplementary information, acknowledgements, peer review information; details of author contributions and competing interests; and statements of data and code availability are available at <https://doi.org/10.1038/s41586-023-06468-9>.

1. Schiermeier, Q. Droughts, heatwaves and floods: how to tell when climate change is to blame. *Nature* **560**, 20–22 (2018).
2. Otto, F. et al. The attribution question. *Nat. Clim. Change* **6**, 813–816 (2016).
3. Philip, S. et al. A protocol for probabilistic extreme event attribution analyses. *Adv. Stat. Climatol. Meteorol. Oceanogr.* **6**, 177–203 (2020).
4. Raju, E., Boyd, E. & Otto, F. Stop blaming the climate for disasters. *Commun. Earth Environ.* **3**, 1 (2022).
5. Lahsen, M. & Ribot, J. Politics of attributing extreme events and disasters to climate change. *Wiley Interdiscip. Rev. Clim. Change* **13**, e750 (2022).
6. Hallegatte, S., Vogt-Schilb, A., Bangalore, M. & Rozenberg, J. *Unbreakable: Building the Resilience of the Poor in the Face of Natural Disasters* (World Bank, 2017).
7. Tellman, B. et al. Satellite imaging reveals increased proportion of population exposed to floods. *Nature* **596**, 80–86 (2021).
8. Henderson, J. V. Cities and development. *J. Reg. Sci.* **50**, 515–540 (2010).
9. Rosenthal, S. S. & Strange, W. C. in *Handbook of Regional and Urban Economics* Vol. 4 (eds Henderson, J. V. & Thisse, J.-F.) 2119–2171 (Elsevier, 2004).
10. Duranton, G. & Puga, D. in *Handbook of Regional and Urban Economics* Vol. 4 (eds Henderson, J. V. & Thisse, J.-F.) 2063–2117 (2004).
11. Neumann, B., Vafeidis, A. T., Zimmermann, J. & Nicholls, R. J. Future coastal population growth and exposure to sea-level rise and coastal flooding - a global assessment. *PLoS One* **10**, e0118571 (2015).
12. Peduzzi, P., Dao, H., Herold, C. & Mouton, F. Assessing global exposure and vulnerability towards natural hazards: the Disaster Risk Index. *Nat. Hazards Earth Syst. Sci.* **9**, 1149–1159 (2009).
13. de Brujin, J. A. et al. A global database of historic and real-time flood events based on social media. *Sci. Data* **6**, 311 (2019).
14. Muis, S., Verlaan, M., Winsemius, H. C., Aerts, J. C. & Ward, P. J. A global reanalysis of storm surges and extreme sea levels. *Nat. Commun.* **7**, 11969 (2016).
15. Rentschler, J., Salhab, M. & Jafino, B. A. Flood exposure and poverty in 188 countries. *Nat. Commun.* **13**, 3527 (2022).
16. Arnell, N. W. & Gosling, S. N. The impacts of climate change on river flood risk at the global scale. *Clim. Change* **134**, 387–401 (2016).
17. Dottori, F. et al. Increased human and economic losses from river flooding with anthropogenic warming. *Nat. Clim. Change* **8**, 781–786 (2018).
18. Andreadis, K. et al. Urbanizing the floodplain: global changes of imperviousness in flood-prone areas. *Environ. Res. Lett.* **17**, 104024 (2022).
19. Smith, A. et al. New estimates of flood exposure in developing countries using high-resolution population data. *Nat. Commun.* **10**, 1814 (2019).
20. Kocornik-Mina, A., McDermott, T. K. J., Michaels, G. & Rauch, F. Flooded cities. *Am. Econ. J. Appl. Econ.* **12**, 35–66 (2020).
21. Winsemius, H. et al. Global drivers of future river flood risk. *Nat. Clim. Change* **6**, 381–385 (2016).
22. Hirabayashi, Y. et al. Global flood risk under climate change. *Nat. Clim. Change* **3**, 816–821 (2013).
23. Jongman, B., Ward, P. & Aerts, J. Global exposure to river and coastal flooding: long term trends and changes. *Glob. Environ. Change* **22**, 823–835 (2012).
24. Tiggeloven, T. et al. Global-scale benefit–cost analysis of coastal flood adaptation to different flood risk drivers using structural measures. *Nat. Hazards Earth Syst. Sci.* **20**, 1025–1044 (2020).
25. Cao, W. et al. Increasing global urban exposure to flooding: an analysis of long-term annual dynamics. *Sci. Total Environ.* **817**, 153012 (2022).
26. Fang, J., Zhang, C., Fang, J., Liu, M. & Luan, Y. Increasing exposure to floods in China revealed by nighttime light data and flood susceptibility mapping. *Environ. Res. Lett.* **16**, 104044 (2021).
27. Shi, J., Cui, L. & Tian, Z. Spatial and temporal distribution and trend in flood and drought disasters in East China. *Environ. Res.* **185**, 109406 (2020).
28. Wang, Y. et al. Spatio-temporal changes of exposure and vulnerability to floods in China. *Adv. Clim. Change Res.* **5**, 197–205 (2014).
29. Du, S., He, C., Huang, Q. & Shi, P. How did the urban land in floodplains distribute and expand in China from 1992–2015? *Environ. Res. Lett.* **13**, 034018 (2018).
30. Dilling, L. et al. Is adaptation success a flawed concept? *Nat. Clim. Change* **9**, 572–574 (2019).
31. Rentschler, J. et al. *Resilient Shores: Vietnam's Coastal Development Between Opportunity and Disaster Risk* (World Bank, 2020).
32. Lin, Y., McDermott, T. K. J. & Michaels, G. Cities and the Sea Level. CESifo Working Papers No. 8997. [https://papers.ssrn.com/sol3/papers.cfm?abstract\\_id=3827610](https://papers.ssrn.com/sol3/papers.cfm?abstract_id=3827610) (2021).
33. Hallegatte, S. How Economic Growth and Rational Decisions Can Make Disaster Losses Grow Faster Than Wealth. Policy Research Working Paper 5617. World Bank Group <https://doi.org/10.1596/1813-9450-5617> (2011).

**Publisher's note** Springer Nature remains neutral with regard to jurisdictional claims in published maps and institutional affiliations.

Springer Nature or its licensor (e.g. a society or other partner) holds exclusive rights to this article under a publishing agreement with the author(s) or other rightsholder(s); author self-archiving of the accepted manuscript version of this article is solely governed by the terms of such publishing agreement and applicable law.

© The World Bank, under exclusive licence to Springer Nature Limited 2023

## Methods

We summarize the data, methods and sensitivity checks that are used in this study to track the speed and shape of settlement expansion and estimate flood exposure.

### Flood-hazard data

One study using coarse flood data projected that the global number of flood-exposed people will reach 1.3 billion by 2050 (ref. 28), but a more recent high-resolution study showed that this threshold has already been exceeded by at least 39% in 2020 (ref. 15). This shows the importance of using high-resolution data to capture the highly localized nature of flood hazards and tendency of people to avoid settling in the most hazardous locations<sup>19</sup>.

This study considers the three most common flood types, which can all contribute to urban flood hazards: fluvial flooding, when intense or excessive precipitation or snowmelt cause rivers to overflow; pluvial flooding, when surface water builds up beyond the absorptive capacity of soil, owing to extended precipitation and insufficient drainage; and coastal flooding, owing to waves, tides, storm surges and sea-level changes.

Country-level pluvial and fluvial flood data are based on the 2019 Fathom Global flood-hazard dataset<sup>34,35</sup>, which is used extensively in the literature<sup>15,18,19,36</sup>. These flood data have been validated in detailed case studies, including for the USA, Canada and the UK<sup>34,37</sup>, as well as a validation study for Nigeria and Mozambique<sup>38</sup>, which finds accuracy rates that are aligned with or only marginally lower than values reported for the UK, Canada and the USA. These flood data provide gridded information on flood extents and depths at a 3-arcsec resolution (equivalent to 90 m at the equator), simulating 5-year, 20-year, 50-year, 100-year, 250-year and 500-year flood events, and are available for all countries. The maps are based on MERIT DEM that corrects for several errors, including absolute bias, stripe noise, speckle noise, and tree and building-height biases, and has been validated extensively<sup>39</sup>. We consider flooding with a 100-year return period in the main study, as well as 5-year, 20-year, 500-year and 1,000-year return periods as a sensitivity test.

In addition, we use a global coastal flood map developed according to refs. 40,41. The dataset has 3-arcsec spatial resolution, generated using the LISFLOOD-FP hydrological model<sup>36</sup>, with MERIT DEM as an input<sup>39</sup>. Coastal flood simulations are forced by extreme sea-level scenarios derived from reanalysing waves (using the WAVEWATCH III model<sup>42</sup>) and storm surges (using the DFlow-FM model<sup>20</sup>), combined with tidal information<sup>40,41</sup>. As with fluvial and pluvial floods, we consider 100-year events, as well as 5-year, 20-year, 500-year and 1,000-year return periods as a sensitivity test.

Global flood maps used in this study do not incorporate the effects of artificial flood-protection structures, such as dykes. This data limitation is pervasive in the literature, as there is no complete global inventory of flood defenses<sup>15</sup>. Continuing initiatives, such as the FLOPROS database, could eventually fulfil this need, but are still falling short of comprehensive coverage<sup>43</sup>. The use of undefended flood maps is likely to result in overestimating exposure in locations in which flood-protection systems defend against 100-year floods (or higher). Case studies and World Bank country risk assessments suggest that most flood-exposed people in LICs and LMICs have no protection from a 100-year flood<sup>31</sup>. Many LICs lack even basic drainage systems to manage light flooding. It is likely that only HICs and some UMICs offer such flood-protection standards to a substantial share of their populations; however, frequent flood disasters in these countries also demonstrate that coverage is far from complete.

This study considers a 1-in-100-year return flood intensity to reflect relatively rare and intense disasters. Further return periods (1-in-5, 1-in-20, 1-in-500 and 1-in-1,000 years) are used for the purpose of robustness tests. However, the concept of return periods is easily

misunderstood and the probability underestimated. A 1-in-100-year flood has, on average, a 1% probability of occurrence in any given year, which translates to a 10% probability in a decade or 50% in a lifetime (68 years). These are notable probabilities that lie well within government planning horizons. For comparison, the Dutch flood-protection system protects against events up to 1-in-10,000 years. Furthermore, these probabilities apply to any given river basin or microclimate (and we consider hundreds of thousands of locations for this study). This means that, globally, hundreds of 1-in-100-year flood events happen every year.

Flood hazards are assumed to be time-invariant during the analysis period, as no time-varying flood-hazard datasets are available. Historic flood-event inventories exist but tend to miss events and only identify areas affected by floods, not those potentially at risk or affected by floods before being settled. In practice, variation in flood-hazard patterns may be because of natural processes (such as interdecadal climate variability) or exacerbated by human interference (such as land-use changes and hydrological infrastructure). Such variation is partly stochastic and may increase or decrease flood hazards in any given location<sup>44</sup>. However, changes in flood-hazard patterns during the analysis period are likely to be small relative to changes in exposure and relative to the overall hazard.

### Global settlement footprint data since 1985

Although satellite imagery is now widely used to understand the spatial patterns of urban development across the world, most datasets only cover the most recent years. The Global Human Settlements Layers were seminal as they produced global urban footprints for four discrete time steps—1975, 1990, 2000 and 2014 (ref. 45); however, inaccuracies and large time gaps between observations limit the insights into the rapid dynamics of urbanization patterns<sup>46</sup>.

Annual high-resolution settlement footprint data are crucial for monitoring the evolution of exposure of people to natural hazards. In this study, we use the WSF-Evo dataset developed by the DLR<sup>47,48</sup>, which enables us to track the flood exposure of new urban development in cities and small rural settlements alike. WSF-Evo outlines the global settlement extent from 1985 to 2015 on a yearly basis at about 30 × 30-m resolution based on archived Landsat imagery, although it does not provide population density information. For each year, we gather all available Landsat 5 and Landsat 7 scenes acquired over the given area of interest and extract key statistics—temporal mean, standard deviation, minimum and maximum—for different spectral indices after performing cloud and cloud-shadow masking. Among others, these include: the normalized difference built-up index (NDBI), the normalized difference vegetation index (NDVI) and the modified normalized difference water index (MNDWI). Temporal features proved to be generally robust if computed over at least seven clear cloud-free/cloud-shadow-free observations. Accordingly, if this constraint is not satisfied for a given pixel in the target year, we enlarge the time frame backwards (at 1-year steps) until the condition is met.

The 2015 edition of WSF-Evo, generated by jointly exploiting both optical (Landsat 8) and radar (Sentinel-1) multitemporal satellite imagery, outlines the global settlement extent at 10 × 10-m resolution<sup>47</sup>. Starting backwards from the 2015 reference extent, we iteratively extract settlement and non-settlement training samples for the given target year  $t$  by applying morphological filtering to the settlement mask derived for the year  $t + 1$ , excluding potentially mislabelled samples by adaptively thresholding the temporal mean NDBI, MNDWI and NDVI. On the basis of the assumption that settlement growth occurred over time, we also disregard all pixels categorized as non-settlement in the WSF2015 from the analysis. Finally, we apply binary random forest classification.

To assess the accuracy of the dataset, we conduct an extensive validation exercise by crowdsourcing photointerpretation of high-resolution airborne and satellite historical imagery, with the support of Google. For this purpose, we define a statistically robust and transparent protocol:

# Article

for 1990, 1995, 2000, 2005, 2010 and 2015, we label about 200,000 30 × 30-m reference cells distributed over 100 sites around the world, summing to about 1.2 million validation samples overall. The results confirm that WSF-Evo shows higher levels of accuracy relative to other global settlement layers—in particular, global human settlement layers (GHSL), global impervious surface areas (GISA), global artificial impervious areas (GAIA) and global annual urban dynamics (GAUD)—thus suggesting that WSF-Evo is well suited for tracking settlement trends in both urban and rural areas. Kappa coefficients for WSF-Evo and comparator layers are explained and presented in detail in the Supplementary Information considering three different assessment criteria.

Availability of Landsat 5 and Landsat 7 imagery varies considerably across the world and over time. Independently from the implemented approach, this may result in inaccuracy of settlement outlines in which we collect few or no scenes. Accordingly, to measure the goodness of the Landsat imagery, we generate an Input Data Consistency (IDC) score, in which: 6 = very good; 5 = good; 4 = fair; 3 = moderate; 2 = low; and 1 = very low. The IDC score is defined as:

$$\text{IDC score} = 7 - \min\{(8 - \min\{\#\text{clearObs}, 7\}) \cdot \min\{6, (\#\text{timeFrame})\}\}, 6\}$$

in which `#clearObs` represents the number of available clear observations per pixel and `#timeFrame` is the corresponding time frame in number of years. Extended Data Fig. 4b shows the IDC score for the global dataset.

To overcome possible drawbacks from settlement overestimation/underestimation owing to limited Landsat data availability before 2000, we apply shape prescriptive modelling (SPM) to the temporal settlement extent profile computed for each subnational unit. SPM allows the model choice and its mathematical form to be driven by an understanding of the underlying process—for example, exhibiting a monotonically decreasing trend or requiring the curve to pass through a given data point. By transforming previous knowledge into a constraint in the modelling function, SPM avoids overfitting. The more we know about a physical phenomenon, the more accurate the functional form will be. We implement SPM to model the settlement extent using least square cubic splines, which offer high flexibility in building a curve. Specifically, the method enables us to: (1) force monotone increasing, as WSF-Evo has been generated assuming settlement growth, and (2) perform a weighted minimization based on the average IDC score, which increases trust in the items corresponding to years with higher data availability.

Lower IDC score values mostly occur before 2000, given the sole availability of Landsat 5 and the limited number of international ground stations capable of receiving Landsat data at that time. We first aggregate the original standard error figures at the subnational level for all 3,307 units and afterwards apply the SPM approach to each of the resulting standard error growth curves, which helps overcome inconsistent trends in years with poor data quality. The yearly IDC score averages computed for each subnational unit are used as weights. Overall, we use SPM to model the temporal profile of the settlement of each subnational unit for the five hazard classes and four flood hazards (that is, pluvial, fluvial, coastal and combined), summing to more than 66,000 curves.

## Administrative boundaries

Our definition of national and subnational boundaries follows the standard World Bank global administrative map. Overall, this study covers 225 countries and territories, which are disaggregated into 3,307 subnational units. Country groupings are also in line with World Bank definitions of geographical regions and income groups (based on their 2015 GDP per capita levels).

## Overlaying annual urbanization and flood-hazard data

This study estimates the share of the world's urbanized land that is exposed to high flood-hazard levels and assesses how this exposure

is evolving over time. Using high-resolution global datasets for flood hazards and settlement extents allows us to conduct this analysis for 225 countries and territories, disaggregated into 3,307 subnational units. This represents the population of the whole world, except those living in disputed territories. The results presented here are derived through a computational workflow that processes large quantities of spatial data, which we can simplify into the following analytical steps:

Step 1. We identify built-up areas using the WSF-Evo dataset, which categorizes each 30 × 30-m resolution pixel as settlement or non-settlement on a yearly basis from 1985 to 2015.

Step 2. We assign each settlement pixel to one of the five considered flood-hazard categories defined in line with risk to lives and livelihoods (Extended Data Table 2). We repeat this step for all of the world's settlements and each year.

Step 3. On a yearly basis, we compute the total settlement area per flood-hazard category for each subnational administrative unit (such as state or province) and calculate its share relative to the corresponding overall settlement area. To address possible limitations of settlement overestimation/underestimation owing to poor Landsat 5 data availability before 2000 in some parts of the world, we apply SPM (see above). To obtain wider trends, we further aggregate exposure estimates to national and regional levels and compute the long-term trends of settlement exposure to flood hazards. When appropriate, estimates are rounded.

## Robustness of estimates

The absolute settlement flood exposure estimates in this study are sensitive to the choice of inundation depth thresholds (Extended Data Table 2). The results presented in this study focus in particular on inundation depths over 0.5 m, thus highlighting areas with high-impact floods. However, there is evidence that flood depths of just 0.15 m can already cause substantial disruptions to economic activity and livelihoods<sup>31</sup>. A sensitivity analysis conducted for this study shows how reducing the depth threshold changes the total exposed settlement area (Extended Data Fig. 4). In line with previous studies, we find that pluvial floods are more sensitive to the choice of threshold, especially at low inundation depths<sup>15</sup>.

In relative terms, this study shows that flood-exposed settlement growth is faster than flood-safe growth. Figure 2d–f shows that this finding is robust to considering combined flood hazards or pluvial, fluvial and coastal floods individually. Year-on-year growth rates (Fig. 2c) demonstrate that this trend is also consistent over time. Moreover, the finding is robust to considering different flood intensities (represented by 5-year, 20-year, 100-year, 500-year and 1,000-year return periods). In China and Vietnam, which together account for 53% of global settlement expansion in high-hazard flood zones, settlement expansion in high-hazard and very-high-hazard zones is consistently faster than in flood-safe zones (Extended Data Fig. 4c,d). In short, the relative speed of settlement growth in flood-exposed and flood-safe areas is robust across flood types, return periods, time and inundation depth thresholds.

## Reporting summary

Further information on research design is available in the Nature Portfolio Reporting Summary linked to this article.

## Data availability

The WSF-Evo dataset is publicly available for download from <https://geoservice.dlr.de/web/maps/eoc:wsfevolution>. We use proprietary global fluvial and pluvial flood-hazard data with the permission of Fathom Global, who provide the data for academic purposes and can be contacted at <https://www.fathom.global/contact-us/>. We use coastal flood maps developed by Vousdoukas et al.<sup>40</sup>, which are publicly available for download from <https://doi.org/10.5281/zenodo.8057902>. Country-level

summary results and subnationally and annually disaggregated results are provided in the Supplementary Information to this study.

## Code availability

The source code for this study is available at <https://doi.org/10.5281/zenodo.7987230>.

34. Sampson, C. C. et al. A high-resolution global flood hazard model. *Water Resour. Res.* **51**, 7358–7381 (2015).
35. Smith, A., Sampson, C. & Bates, P. Regional flood frequency analysis at the global scale. *Water Resour. Res.* **51**, 539–553 (2015).
36. Koks, E. E. et al. A global multi-hazard risk analysis of road and railway infrastructure assets. *Nat. Commun.* **10**, 2677 (2019).
37. Wing, O. E. J. et al. Validation of a 30 m resolution flood hazard model of the conterminous United States. *Water Resour. Res.* **53**, 7968–7986 (2017).
38. Bernhofen, M. V. et al. A first collective validation of global fluvial flood models for major floods in Nigeria and Mozambique. *Environ. Res. Lett.* **13**, 104007 (2018).
39. Yamazaki, D. et al. A high-accuracy map of global terrain elevations. *Geophys. Res. Lett.* **44**, 5844–5853 (2017).
40. Vousdoukas, M. I. et al. Global probabilistic projections of extreme sea levels show intensification of coastal flood hazard. *Nat. Commun.* **9**, 2360 (2018).
41. Vousdoukas, M. I. et al. Developments in large-scale coastal flood hazard mapping. *Nat. Hazards Earth Syst. Sci.* **16**, 1841–1853 (2016).
42. Tolman, H. L. User Manual and System Documentation of WAVEWATCH III version 3.14. Technical note. MMAB Contribution No. 276, 220 pp (2009).
43. Scussolini, et al. FLOPROS: an evolving global database of flood protection standards. *Nat. Hazards Earth Syst. Sci.* **16**, 1049–1061 (2016).
44. Blöschl, G. et al. Changing climate both increases and decreases European river floods. *Nature* **573**, 108–111 (2019).
45. Corbane, C., Florczyk, A., Pesaresi, M., Politis, P. & Syrris, V. GHS-BUILT R2018A - GHS built-up grid, derived from Landsat, multitemporal (1975-1990-2000-2014). European Commission, Joint Research Centre <https://doi.org/10.2905/jrc-ghsl-10007> (2018).
46. Liu, X. et al. High-spatiotemporal-resolution mapping of global urban change from 1985 to 2015. *Nat Sustain.* **3**, 564–570 (2020).
47. Marconcini, M., Metz-Marconcini, A., Esch, T. & Gorelick, N. Understanding current trends in global urbanisation – the World Settlement Footprint suite. *Gl\_Forum* **9**, 33–38 (2021).
48. German Aerospace Center (DLR). EOC Geoservice <https://geoservice.dlr.de/web/maps/eoc:wsfevolution> (2021).

**Acknowledgements** This study has benefited from feedback and input by L. Bernard, R. Damania, V. Deparday, K. Garrett, C. Gevaert, N. Holm-Nielsen, B. Jongman, N. Lozano Gracia, S. Ramesh, C. Riom and L. Southwood. It was supported by the Global Facility for Disaster Reduction and Recovery (GFDRR).

**Author contributions** J.R. and P.A. led the conception, study design, analysis and drafting, with input from S.H., R.S. and M.M. M.M. and E.S. developed the WSF-Evo dataset, designed and implemented the computational process and performed sensitivity tests. M.V. developed the coastal flood-hazard data and performed sensitivity tests. All authors critically revised the manuscript and gave final approval for publication.

**Competing interests** The authors declare no competing interests.

## Additional information

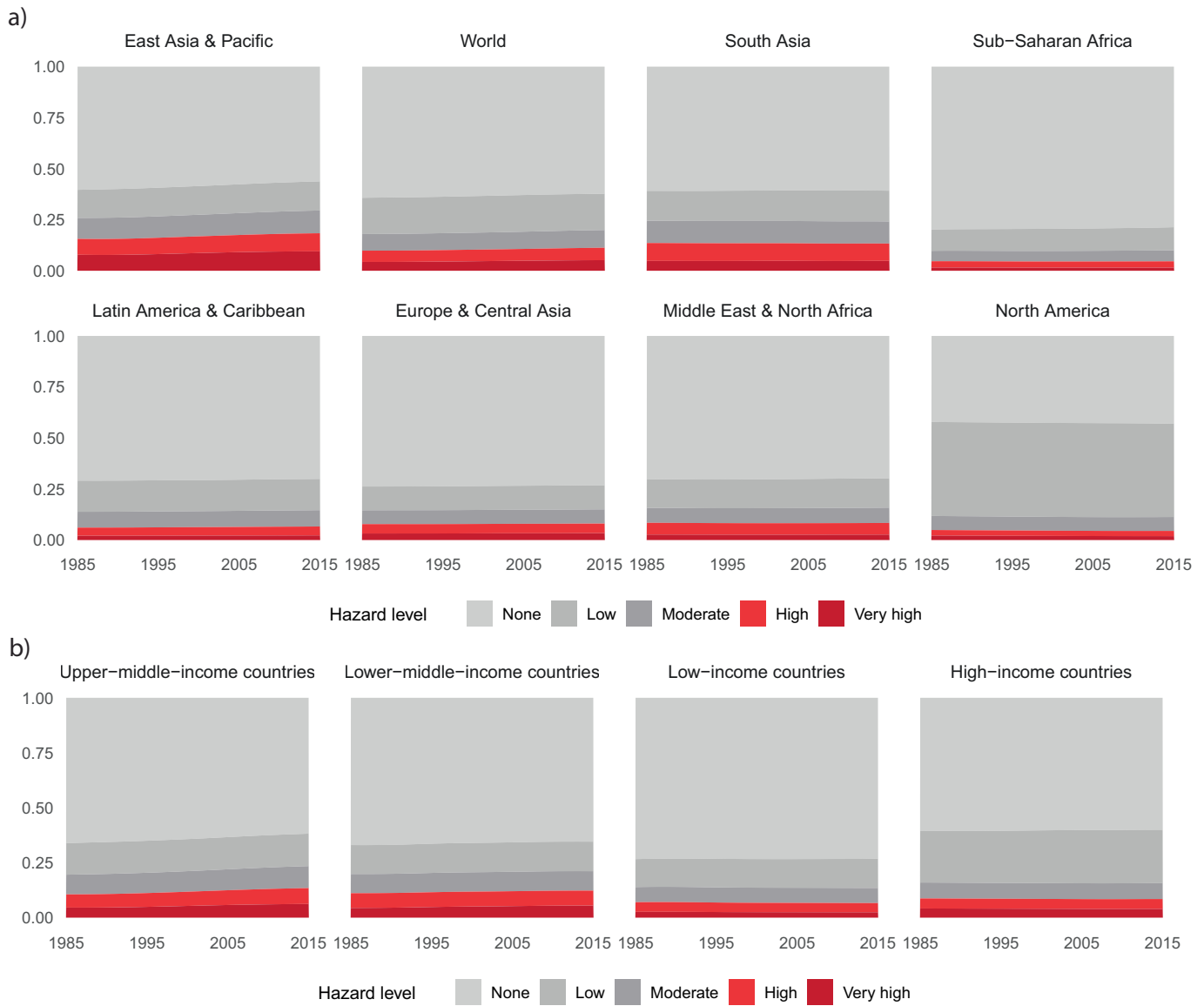
**Supplementary information** The online version contains supplementary material available at <https://doi.org/10.1038/s41586-023-06468-9>.

**Correspondence and requests for materials** should be addressed to Jun Rentschler.

**Peer review information** *Nature* thanks Thomas Corringham, Long Yang and the other, anonymous, reviewer(s) for their contribution to the peer review of this work. Peer reviewer reports are available.

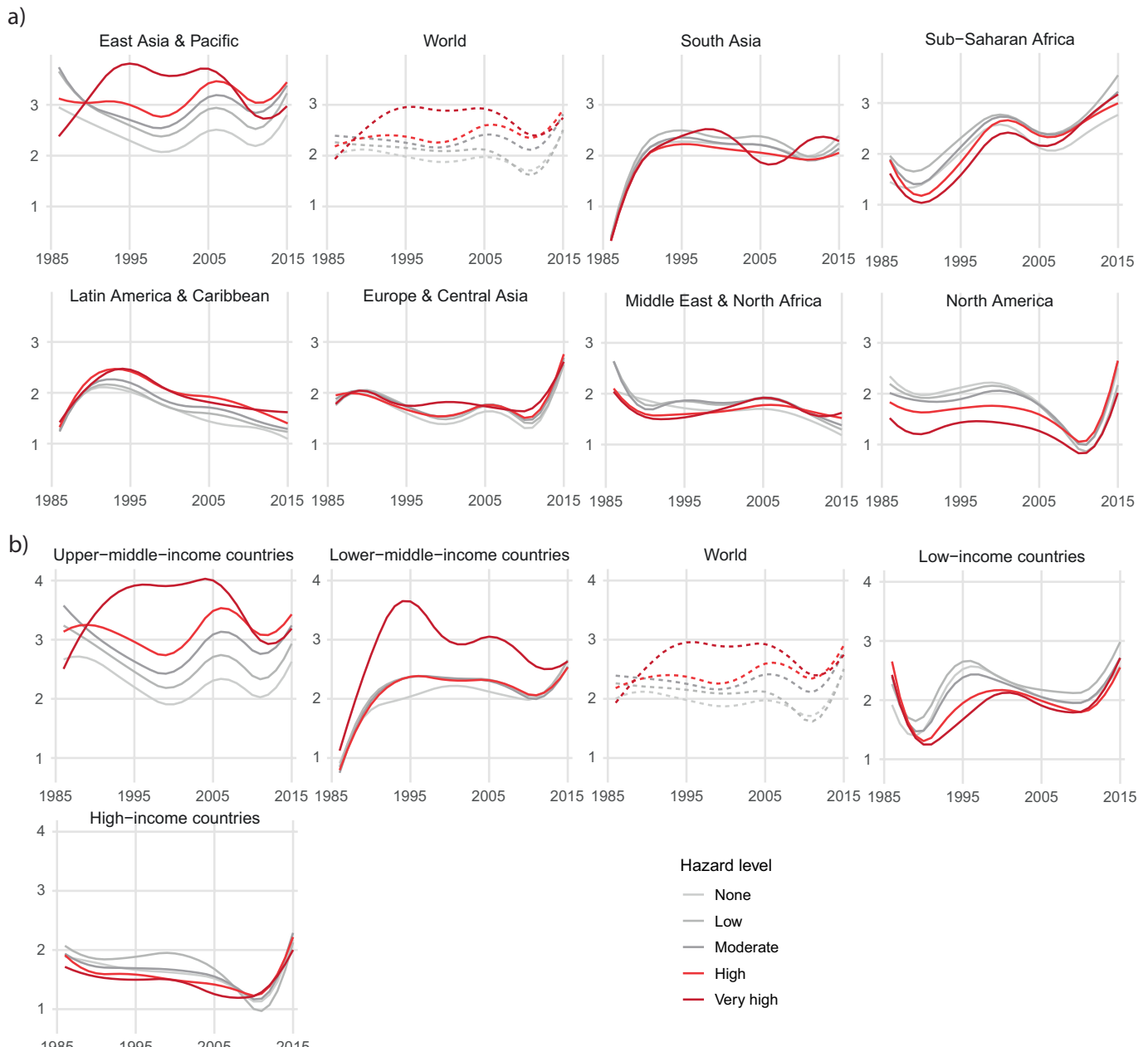
**Reprints and permissions information** is available at <http://www.nature.com/reprints>.

# Article



**Extended Data Fig. 1 | Flood-exposed settlement extents as a share of overall settlements over time.** a, By region, settlement extent, normalized. b, By income group, settlement extent, normalized. Hazard classes are defined

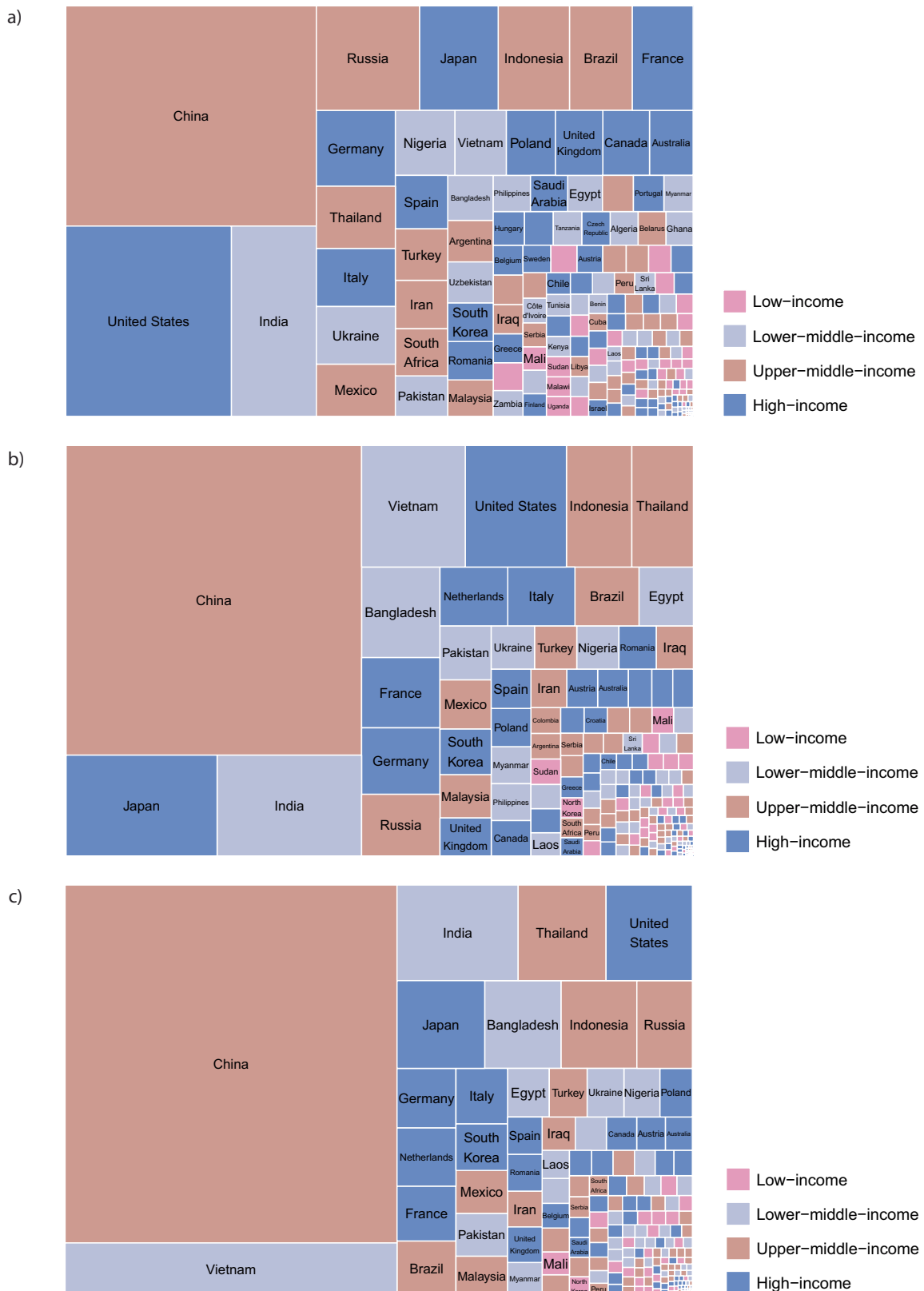
on the basis of the estimated inundation depth experienced during a 1-in-100-year flood: none (flood depths of 0 cm), low (up to 15 cm), moderate (between 15 and 50 cm), high (between 50 and 150 cm) and very high (over 150 cm).



**Extended Data Fig. 2 | Year-on-year settlement growth (%).** a, By region. b, By income groupings. Hazard classes are defined on the basis of the estimated inundation depth experienced during a 1-in-100-year flood: none (flood depths

of 0 cm), low (up to 15 cm), moderate (between 15 and 50 cm), high (between 50 and 150 cm) and very high (over 150 cm).

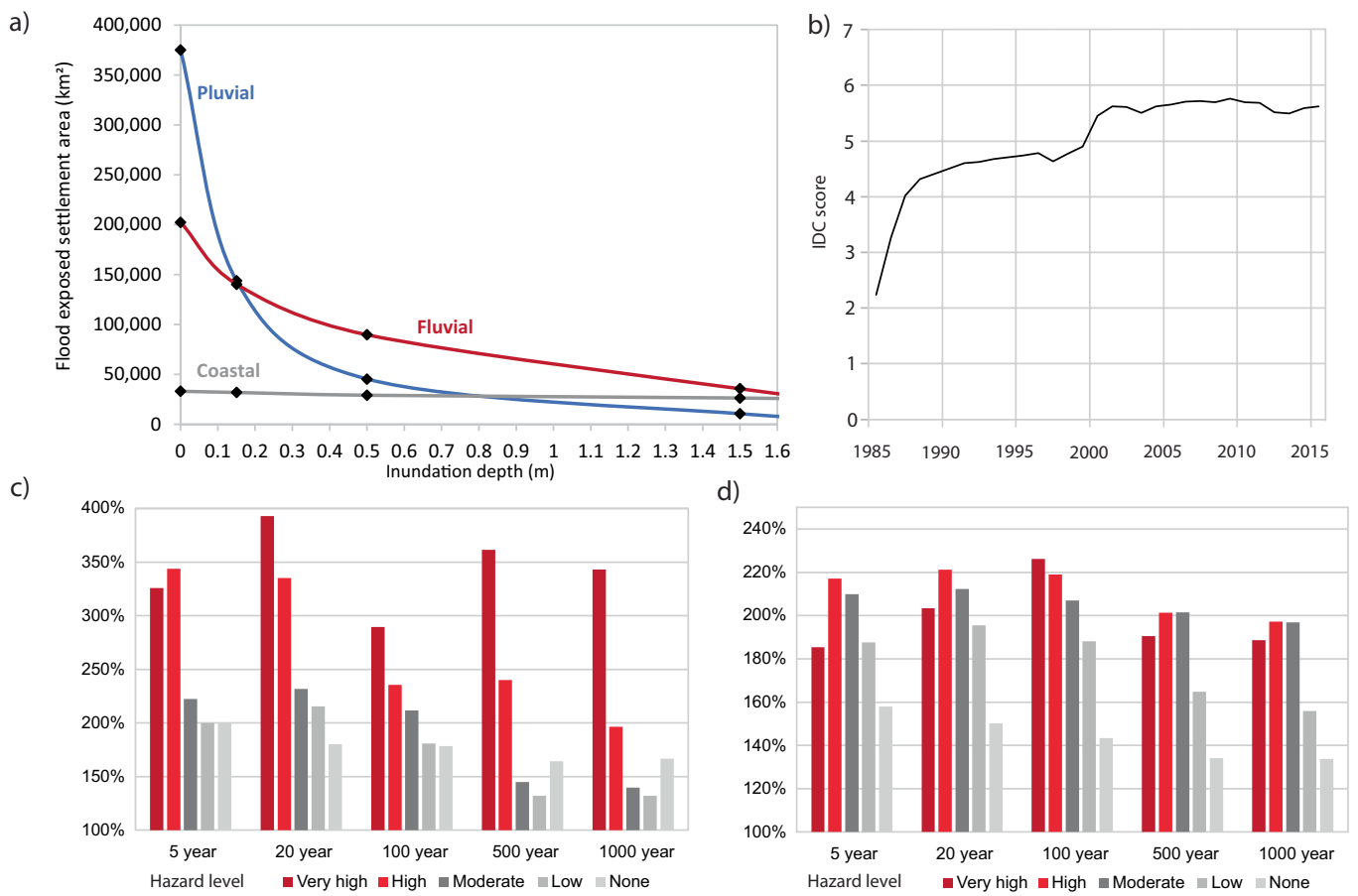
## Article



### **Extended Data Fig. 3 | Proportional representation of settlement extent.**

**a**, Global settlement (1.3 million km<sup>2</sup> total in 2015). **b**, Settlement extent in high-hazard flood areas (144,600 km<sup>2</sup> total in 2015). **c**, New settlement extent in high-hazard flood areas (76,400 km<sup>2</sup> total during 1985–2015). These figures

offer proportional representations of settlement areas in different countries. In each subfigure, the sum of all tiles corresponds to the total settlement extent (in km<sup>2</sup>) specified in parentheses.



**Extended Data Fig. 4 | Sensitivity and robustness of estimates.** **a**, Flood-exposed settlement area for different inundation depth thresholds. **b**, IDC score. **c**, Vietnam: settlement expansion by hazard zones and flood return

periods (1985–2015). **d**, China: settlement expansion by hazard zones and flood return periods (1985–2015).

# Article

**Extended Data Table 1 | Changing flood exposure in the world's built-up areas**

		Global settlement extent	Share (%) of global settlements facing... <i>(Inundation depth during 100-year flood)</i>				
			...no hazard (0 m)	...low hazard (0, 0.15 m]	...medium hazard (0.15, 0.5 m]	...high hazard (0.5, 1.5 m]	...very high hazard 
<b>1985</b>	%	100	64.2	17.8	8.1	5.5	4.3
	km <sup>2</sup> ('000)	693	445	123	56	38	30
<b>2015</b>	%	100	62.3	17.8	8.7	6.1	5.2
	km <sup>2</sup> ('000)	1,284	799	228	112	78	66
<b>Change</b>	<i>Percentage points</i>		-1.9	0	0.6	0.6	0.9

**Extended Data Table 2 | Flood-hazard categorization applied in this study**

Category	Hazard class	Flood depth (meters)	Description
0	None	0	Unaffected during a 1-in-100 year flood
1	Low	0 – 0.15	No significant risk to life or economic activity
2	Moderate	0.15 – 0.5	Disruptions to livelihoods and economic activity; some risk to life for select populations, especially vulnerable groups such as children and disabled people (including through water-borne diseases)
3	High	0.5 – 1.5	A significant share of the affected population is expected to face risk to life, especially if flood waters have a current; major disruptions to livelihoods
4	Very high	Over 1.5	Most affected people could face substantial risk to life and severe and prolonged disruptions to livelihoods

Corresponding author(s): Jun Rentschler

Last updated by author(s): Jun 20, 2023

## Reporting Summary

Nature Portfolio wishes to improve the reproducibility of the work that we publish. This form provides structure for consistency and transparency in reporting. For further information on Nature Portfolio policies, see our [Editorial Policies](#) and the [Editorial Policy Checklist](#).

### Statistics

For all statistical analyses, confirm that the following items are present in the figure legend, table legend, main text, or Methods section.

n/a Confirmed

- The exact sample size ( $n$ ) for each experimental group/condition, given as a discrete number and unit of measurement
- A statement on whether measurements were taken from distinct samples or whether the same sample was measured repeatedly
- The statistical test(s) used AND whether they are one- or two-sided  
*Only common tests should be described solely by name; describe more complex techniques in the Methods section.*
- A description of all covariates tested
- A description of any assumptions or corrections, such as tests of normality and adjustment for multiple comparisons
- A full description of the statistical parameters including central tendency (e.g. means) or other basic estimates (e.g. regression coefficient) AND variation (e.g. standard deviation) or associated estimates of uncertainty (e.g. confidence intervals)
- For null hypothesis testing, the test statistic (e.g.  $F$ ,  $t$ ,  $r$ ) with confidence intervals, effect sizes, degrees of freedom and  $P$  value noted  
*Give P values as exact values whenever suitable.*
- For Bayesian analysis, information on the choice of priors and Markov chain Monte Carlo settings
- For hierarchical and complex designs, identification of the appropriate level for tests and full reporting of outcomes
- Estimates of effect sizes (e.g. Cohen's  $d$ , Pearson's  $r$ ), indicating how they were calculated

*Our web collection on [statistics for biologists](#) contains articles on many of the points above.*

### Software and code

Policy information about [availability of computer code](#)

Data collection No new primary data were collected, hence no data collection software was used.

Data analysis All data analysis was conducted using open source software: Data processing was conducted using Python 3.6,

Visualizations for this study were produced using QGIS 3.16.

The generation of the flood hazard maps used in this study relies on the models LISFLOOD-FP, DEM MERIT, WAVEWATCH-III, and DFLOW-FM.

For manuscripts utilizing custom algorithms or software that are central to the research but not yet described in published literature, software must be made available to editors and reviewers. We strongly encourage code deposition in a community repository (e.g. GitHub). See the Nature Portfolio [guidelines for submitting code & software](#) for further information.

### Data

Policy information about [availability of data](#)

All manuscripts must include a [data availability statement](#). This statement should provide the following information, where applicable:

- Accession codes, unique identifiers, or web links for publicly available datasets
- A description of any restrictions on data availability
- For clinical datasets or third party data, please ensure that the statement adheres to our [policy](#)

We use global fluvial and pluvial flood hazard data (July 2020 version) with the permission of Fathom Global. Available from: <https://www.fathom.global/product/>

flood-hazard-data-maps/global-flood-map/

The coastal flood hazard data were developed based on Vousdoukas et al (2018) and are publicly available for download from <https://doi.org/10.5281/zenodo.8057902>.

The WSF-Evo dataset is publicly available for download from this platform: <https://geoservice.dlr.de/web/maps/eoc:wsfevolution>

## Human research participants

Policy information about [studies involving human research participants](#) and [Sex and Gender in Research](#).

Reporting on sex and gender

n/a

Population characteristics

n/a

Recruitment

n/a

Ethics oversight

n/a

Note that full information on the approval of the study protocol must also be provided in the manuscript.

## Field-specific reporting

Please select the one below that is the best fit for your research. If you are not sure, read the appropriate sections before making your selection.

Life sciences       Behavioural & social sciences       Ecological, evolutionary & environmental sciences

For a reference copy of the document with all sections, see [nature.com/documents/nr-reporting-summary-flat.pdf](https://nature.com/documents/nr-reporting-summary-flat.pdf)

## Ecological, evolutionary & environmental sciences study design

All studies must disclose on these points even when the disclosure is negative.

Study description

This study stands at the nexus of environmental and geographic science. We construct a combined global flood hazard map that depict inundations depths during coastal, fluvial, and pluvial flood events. We overlay this with 30 years of settlement expansion data derived from satellite imagery, indicating built-up locations at the grid cell level with global coverage. The flood hazard exposure of human settlements are then estimated and aggregated to subnational areas, to estimate trends in the hazard exposure of settlement expansion.

Research sample

Our study sample covers all of the world's human settlements. Only a number of small island states and populations in disputed territories are excluded.

Sampling strategy

The WSF-Evo dataset on human settlements has global coverage, i.e. covering all settlements in all countries. From this population we draw our sample by retaining those countries for which flood data and conclusive political boundaries exist. This means several small island states, disputed territories, and areas with missing data inputs were excluded. 218 countries and territories remain in the final sample. The sample is representative of all human settlements in those sampled 218 countries, given some inaccuracy in the image detection process (see sensitivity analysis detailed in the supplementary materials file).

Data collection

Pluvial and fluvial flood maps were developed by Fathom Global. The coastal flood map was developed by one of the co-authors while at the European Commission's JRC. For flood maps, the models LISFLOOD-FP, DEM MERIT, WAVEWATCH-III, and DFLOW-FM were used. Human settlement footprints are from the WSF-Evo dataset produced by DLR and one of this study's co-authors.

Timing and spatial scale

Human settlement footprint data represent the period 1985 to 2015. Flood hazard data represent probabilistic flood hazard conditions in 2019. The spatial scope of the analysis is global (A number of small island states and populations in disputed territories are excluded.).

Data exclusions

Countries or subnational regions were only excluded if one or more of the data inputs were not available. Areas within politically disputed borders were omitted and not assigned to a country.

Reproducibility

Results can be reproduced using the code, which is made available by the authors.

Randomization

No randomization was necessary. We are neither measuring treatment effects nor conducting an experiment.

Blinding

Blinding was not applicable as the study does not involve a treatment or experiment.

Did the study involve field work?

Yes

No

# Reporting for specific materials, systems and methods

We require information from authors about some types of materials, experimental systems and methods used in many studies. Here, indicate whether each material, system or method listed is relevant to your study. If you are not sure if a list item applies to your research, read the appropriate section before selecting a response.

## Materials & experimental systems

n/a	Involved in the study
<input checked="" type="checkbox"/>	Antibodies
<input checked="" type="checkbox"/>	Eukaryotic cell lines
<input checked="" type="checkbox"/>	Palaeontology and archaeology
<input checked="" type="checkbox"/>	Animals and other organisms
<input checked="" type="checkbox"/>	Clinical data
<input checked="" type="checkbox"/>	Dual use research of concern

## Methods

n/a	Involved in the study
<input checked="" type="checkbox"/>	ChIP-seq
<input checked="" type="checkbox"/>	Flow cytometry
<input checked="" type="checkbox"/>	MRI-based neuroimaging